Modelling of Anti-Amyloid-Beta Therapy for Alzheimer's Disease

Pal, S. and Melnik, R.

Proceedings of the IWBBIO 2023 (10th International Work-Conference on Bioinformatics and Biomedical Engineering), I. Rojas et al (Eds), Part I, LNCS 13919, Springer-Nature, 2023.

Modelling of Anti-Amyloid-Beta Therapy for Alzheimer's Disease

Swadesh Pal[1 [0000−0002−6873−7338]] and Roderick Melnik[1,2 [0000−0002−1560−6684]]

[1] M3AI Laboratory, MS2Discovery Interdisciplinary Research Institute, Wilfrid Laurier University, Waterloo, ON, Canada N2L 3C5
[2] BCAM - Basque Center for Applied Mathematics, E-48009, Bilbao, Spain
rmelnik@wlu.ca
http://m3ai.wlu.ca

Abstract. A healthy brain clears different types of debris with the help of specialized glial cells. These cells contiguously tile the entire central nervous system (CNS), exert many essential complex functions in the healthy CNS, and maintain a healthy balance in the brain. However, over age, these cells fail to control the healthy balance of the proteins and cause different neurodegenerative diseases, one of which is Alzheimer's disease (AD). In AD, insoluble amyloid-beta plaques accumulate in the extracellular space along with neurofibrillary tangles (NFTs) inside the brain cells. In this paper, we have developed a model and studied the accumulation of amyloid-beta plaques and NFTs along with an anti-amyloid-beta therapy applied in the treatment of the disease. Based on these studies, we have demonstrated the dynamics of the modelling therapy such that the drug helps clear a subsequent amount of amyloid-beta plaques in each dose. Numerical simulations have been used to show different long-term outcomes of the model. To further analyze the disease progression in the brain and its treatment, we have integrated brain connectome data in the network model as part of our developed modelling framework.

Keywords: Alzheimer's disease, amyloid-beta plaques, phosphorylated tau, drug-controlled treatments, neurodegeneration, cognitive declines, data-driven models, brain connectome

1 Introduction

Alzheimer's disease (AD) is the leading neurodegenerative disease in the current century, and it causes neuronal death in the brain and disables different functional abilities. More than 50 million people worldwide have this dementia, and this number is expected to reach over 150 million in three decades [1]. It is very hard to identify this dementia at the early stage as it slowly develops in the brain. The development of the disease causes damage to the brain, and when it gets noticed, it already affects most parts of the brain. Therefore, it is important to check the disease status on a regular basis. Researchers have been trying to understand the mechanism behind AD progression, but it is still not

fully clear. Not without some controversy, the Food and Drug Administration (FDA) recently granted the first-ever disease-modifying therapy for AD, aducanumab, followed by lecanemab earlier this year. The former one, in particular, is a monoclonal antibody directed against the amyloid-beta protein [2]. Some other approved drugs are available, but none of these drugs prevents neuronal loss [3]. Therefore, disease-modifying therapies play an important role in controlling the brain's AD progression.

While many ingredients participate in AD initiation and progression, the amyloid-beta and tau proteins are widely recognized as the two most active ingredients [4]. Generally, amyloid-beta accumulates in the extracellular space in the form of insoluble plaques, and tau proteins form neurofibrillary tangles (NFTs) inside the brain cells. The normal brain clears these insoluble plaques and NFTs up to a certain level of these productions, but beyond that, these cause disruptions in the normal activities of the brain cell and move towards AD [5]. For instance, specialized glial cells called astrocytes help in clearing amyloid-beta plaques, and they also help in the modulation of memory and learning processes [6–9]. Different disease-modifying therapies support removing some extra amount of these insoluble plaques so that they can maintain a healthy balance in the brain. Applying those in the brain causes side effects, and clinical trials have been going on for some of these therapies. In analyzing a therapy, our better understanding of all the side effects and any necessary modifications of the doses require time. Computational modelling helps researchers in silico trials to go deeper in a limited time and is no exception for AD. Several mathematical models have been developed based on systems biology approaches to AD molecular and cellular pathophysiologic mechanisms [10–13].

Starting with a general reaction-diffusion framework, we have used logistic models for the temporal evolution of amyloid-beta plaques and phosphorylated tau proteins in the brain [2]. In this work, we study the anti-amyloid beta treatment with the help of a newly proposed mathematical model. In addition, we formulate a network mathematical model to integrate the brain connectome data and examine the effect of anti-amyloid beta in the clearance of amyloid-beta plaques in the brain. Each drug has its own reaction time; generally, it increases the body's reaction gradually and then decreases. We have included such types of drug control phenomena in the model. We use different parameter sets estimated by Hao et al. [2] for various typical population groups (e.g., Alzheimer's disease, late mild cognitive impairment, and cognitively normal) captured by the model. We have constructed an anti-amyloid-beta therapy function in the model, which shows a little clearance of amyloid-beta plaques in each dose can help recover from AD in the long term.

The organization of the rest of this paper is as follows. In Section 2, we describe the reaction-diffusion and the network models, which use in the brain connectome consideration in the latter case. Simulation results and their discussions are presented in Section 3 followed by conclusions in Section 4.

2 Model for AD

Amyloid-beta is one of the key factors in Alzheimer's disease. The imbalance between the production and clearance of amyloid-beta causes amyloid-beta plaque accumulation. On the other hand, several studies related to AD show that the accumulation of amyloid-beta plaques enhances the tau protein's phosphorylation. Researchers have been modelling the accumulations of amyloid-beta plaques and the deposition of tau tangles in various mathematical approaches [10–13]; the approach based on partial differential equations is one of them. In this work, we model them with the following system of coupled reaction-diffusion equations [2]:

$$\frac{\partial u}{\partial t} = \nabla \cdot (\mathbf{D}_u \nabla u) + r_u u\left(1 - \frac{u}{K_u}\right), \tag{1a}$$

$$\frac{\partial v}{\partial t} = \nabla \cdot (\mathbf{D}_v \nabla v) + r_v u\left(1 - \frac{v}{K_v}\right), \tag{1b}$$

which we supplement with the non-negative initial conditions $u(\mathbf{x}, T_0) = u_0$ and $v(\mathbf{x}, T_0) = v_0$ at the age T_0. Here, $u(\mathbf{x}, t)$ and $v(\mathbf{x}, t)$ are the densities of amyloid-beta plaques and phosphorylated tau proteins at a spatial point $\mathbf{x} \in \Omega \subset \mathbb{R}^3$ and time t. The first term on the right-hand side in each of the equations incorporates the random movement of the concentrations in the domain Ω. Here, we have considered the diffusion in amyloid-beta plaques because the soluble proteins (oligomers) of amyloid-beta can diffuse through brain tissue [14]. Our coupled model (1) is also supplemented by corresponding boundary conditions. In particular, our results have been obtained under no-flux boundary conditions. The parameters r_u and r_v in (1) are the growth rates of amyloid-beta and tau protein, whereas K_u and K_v are their carrying capacities, respectively. The tau deposition disrupts different cell functions and induces neurodegeneration and cognitive declines. We model this neurodegeneration (n) and cognitive declines (c) by the following equations:

$$\frac{dn}{dt} = r_n v\left(1 - \frac{n}{K_n}\right), \tag{2a}$$

$$\frac{dc}{dt} = (r_{cn} n + r_{cv} v)\left(1 - \frac{c}{K_c}\right), \tag{2b}$$

with non-negative initial conditions $n(\mathbf{x}, T_0) = n_0$ and $c(\mathbf{x}, T_0) = c_0$. Here, r_n is the growth rate of neurodegeneration, and r_{cn} and r_{cv} are the growth rates for cognitive declines due to neurodegeneration and tau protein, respectively. The parameters K_n and K_c in (2) are the carrying capacities for the neurodegeneration and cognitive declines.

2.1 Anti-amyloid-beta treatments

Currently, there is a limited number of drugs available for AD treatments. Most recently, the Food and Drug Administration (FDA) approved several new ones

(in particular, aducanumab), but they do not prevent neuronal loss [3]. Therefore, disease-modifying therapies are important in controlling the brain's AD progression. To study the anti-amyloid-beta therapy, we modify the first equation of (1) to include the drug influence on the evolution of amyloid-beta plaques, leading to:

$$\frac{\partial u}{\partial t} = \nabla \cdot (\mathbf{D}_u \nabla u) + r_u u\left(1 - \frac{u}{K_u}\right) - \Phi(t)u, \tag{3}$$

with the same initial condition as before. The function $\Phi(t)$ represents the drug-control function, which clears the amyloid-beta plaques; it is generally non-constant over time. The drug starts to remove the amyloid-beta plaques after receiving a dosage. The clearance rate increases initially due to the drug, but it begins to decay after some time, landing at a certain level before receiving the next dosage. The AD patient recovers if the latest clearance rate exceeds the previous rate. However, due to the different side effects of drugs (e.g., brain edema and hemorrhage), we can not apply the therapy back-to-back to increase the clearance rate rapidly [15, 16]. Therefore, a slight recovery each time is crucial to achieving the final goal. Taking this into consideration, we can define the drug-control function $\Phi(t)$ between any two dosages T_p and T_{p+1} ($p = 0, 1, 2, \ldots$), which satisfies the differential equation:

$$\frac{d\Phi}{dt} = \lambda(t)\Phi(t), \quad t \in (T_p, T_{p+1}), \tag{4}$$

with the positive initial condition $\Phi(T_0) = \phi_0$ as the natural clearance rate for plaques for a patient before starting the medication. Here, $\lambda(t)$ is the per-capita clearance rate of the drug. We consider this function as $\lambda(t) = \gamma(t_m - t_l(t))$, where γ describes the rate of clearance of plaques and $t_l(t)$ is the time since the last received dosage. The term t_m represents the time when the clearance rate is maximum, which may vary between drug dosages, but we assume it as a constant for simplicity. For each $p \geq 1$, the function $\lambda(t)$ is discontinuous at T_p as $t_l(t) = 0$ for the dosage days. Hence the control function $\Phi(t)$ is not differentiable at those T_p. In addition, we assume the continuity for the control function Φ over the whole time period of the treatment. This approach can also be applied to other treatment plans.

2.2 Network model for the brain connectome

We extend the temporal models defined earlier into a system based on the network model to integrate the brain connectome data [17–21]. This enables us to characterize the dynamics of the ingredients on a spatio-temporal scale. Suppose the brain data are represented by a graph $\mathbf{G}$ with V nodes and E edges. For graph $\mathbf{G}$, we construct the adjacency matrix $\mathbf{A}$, which helps us to assemble the Laplacian on the graph. We define the (i, j) $(i, j = 1, 2, 3, \ldots, V)$ element of the matrix $\mathbf{A}$ as

$$A_{ij} = \frac{n_{ij}}{l_{ij}^2},$$

where n_{ij} is the mean fiber number and l_{ij}^2 is the mean length squared between the nodes i and j. We further define the elements of the Laplacian matrix $\mathbf{L}$ as

$$L_{ij} = D_{ij} - A_{ij}, \quad i, j = 1, 2, 3, \ldots, V,$$

where $D_{ii} = \sum_{j=1}^{V} A_{ij}$ are the elements of the diagonal weighted-degree matrix. Now we can write a network mathematical model on the graph $\mathbf{G}$ with the help of this Laplacian matrix that is given by:

$$\frac{du_j}{dt} = -\rho_u \sum_{k=1}^{V} L_{jk} u_k + r_u u_j \left(1 - \frac{u_j}{K_u}\right) - \Phi(t) u_j, \tag{5a}$$

$$\frac{dv_j}{dt} = -\rho_v \sum_{k=1}^{V} L_{jk} v_k + r_v u_j \left(1 - \frac{v_j}{K_v}\right), \tag{5b}$$

$$\frac{dn_j}{dt} = r_n v_j \left(1 - \frac{n_j}{K_n}\right), \tag{5c}$$

$$\frac{dc_j}{dt} = (r_{cn} n_j + r_{cv} v_j) \left(1 - \frac{c_j}{K_c}\right), \tag{5d}$$

with $\Phi(t)$ satisfying the drug-control equation (4). Here, u_j, v_j, n_j, and c_j denote the concentrations of u, v, n, and c respectively, at the node j. The parameters ρ_u and ρ_v are the diffusion coefficients of amyloid-beta plaques (u) and tau proteins (v), respectively. In the simulations, we use non-negative initial conditions for all the variables.

3 Results and Discussions

In this section, we numerically analyze the model (1) and the anti-amyloid-beta treatment (3). An in-house tool based on Matlab and C-language has been developed and used for the simulations. Authors in [2] estimated the parameter values for the model (1) with integrated therapy (2) for different groups of patients by using cerebrospinal fluid amyloid beta42 biomarker data, and the values are given in Table 1. We use these parameter values in our model along with the drug-control function modified in this work, as described in the previous section.

3.1 Dynamics for the homogeneous system

First, we note that the homogeneous system corresponding to the network model can be obtained by setting the graph Laplacian to zero. Before studying the drug-control model (3), we start with finding some characteristics of drug function for the FDA-approved drug called 'aducanumab'. During the treatment, aducanumab is administered intravenously (IV) via a 45-60 minute infusion every four weeks. After applying it, the drug accelerates the clearance rate of amyloid plaques. The maximum clearance rate must occur at least half-time between two dosages to cure AD, i.e., t_m should be greater than two weeks. We choose

Table 1: The mean initial conditions and parameter values for Alzheimer's disease (AD), late mild cognitive impairment (LMCI) and cognitively normal (CN) groups [2].

Parameter	AD group	LMCI group	CN group
u_0	36.03	41.57	44.92
v_0	12.38	4.21	3.69
n_0	0.26	0.48	0.42
c_0	3.68	6.03	2.58
r_u	18.35×10^{-2}	16.12×10^{-2}	16.82×10^{-2}
K_u	259.44	264.99	276.21
r_v	0.15	0.08	0.12
K_v	123.35	131.66	126.53
r_n	6.90×10^{-3}	7.37×10^{-3}	7.24×10^{-3}
K_n	1.0	1.02	1.03
r_{cn}	1.67	1.26	3.16
r_{cv}	3.83	1.93	2.48
K_c	169.48	129.40	59.89

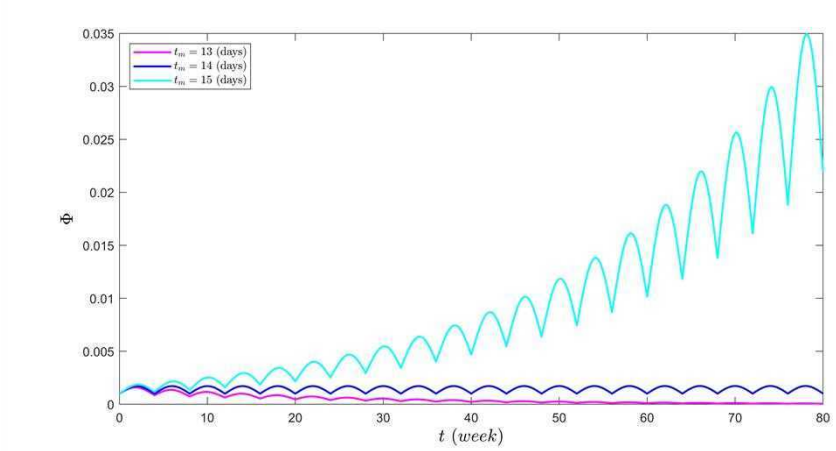

Fig. 1: (Color online) The drug-control function (4) for different t_m with $\gamma = 5.5 \times 10^{-3}$ and $T_p = 4p$ (weeks): magenta - 13 days, blue - 14 days, and cyan - 15 days.

$t_m = 15$ (days) for simulations [see Fig. 1]. On the other hand, based on the aducanumab data released by Biogen, the amyloid PET assessment data at week 78 were decreased by 16.5% compared to the baseline. Using these data and Table 1, we have estimated $\gamma = 5.5 \times 10^{-3}$. We fix $\gamma = 5.5 \times 10^{-3}$ and $t_m = 15$ (days) for all the simulations reported next.

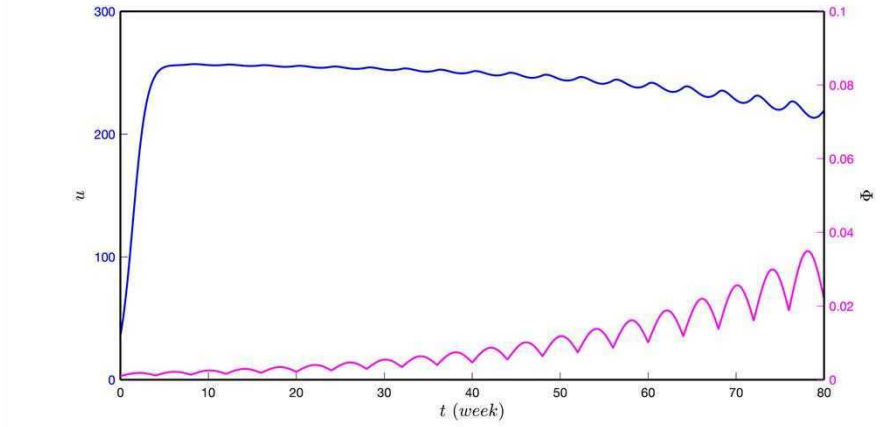

Fig. 2: (Color online) The accumulations of amyloid-beta (blue) for AD group in the presence of drug-control (magenta) with $\gamma = 5.5 \times 10^{-3}, t_m = 15$ (days) and $T_p = 4p$ (weeks). The simulation uses the mean parameter values from Table 1.

Fig. 2 depicts the accumulation of amyloid plaques for the AD patient group in the presence of drug control applied every four weeks. It shows that the drug clears the plaques from the highest level. We plot the solutions for phosphorylated tau and cognitive declines in Fig. 3. These solutions show that the anti-amyloid-beta therapy does not affect the phosphorylated tau and cognitive declines; however, they saturate at their carrying capacities. This happens due to the exponential growth in the accumulation of phosphorylated tau inside the brain cells at the initial stage. In addition, it can be shown that a less phosphorylated tau accumulation if we are able to control its growth before it converges to the saturated value. Furthermore, we have observed the same type of behaviour of the solution of neurodegeneration in the model.

We also plot the accumulation and clearance of plaques for the other groups in Fig. 4. It can be seen that the solution behaviours are almost the same for all the groups. Furthermore, it shows that the drug helps to clear the amyloid-beta plaques for all the groups in the long term. However, this clearance cannot control the accumulation of phosphorylated tau, neurodegeneration and cognitive declines. Other interesting things happen if the patient stops the treatment before or after the recovery. To study these scenarios, we stopped the drug after two and three years [see Fig. 5]. The simulations show that the plaques accumulate and are saturated to the carrying capacity. Therefore, the disease will not disappear permanently and could return if we stop the medication.

3.2 Solution for the network model

We have used brain connectome data for the network model, which is available at https://braingraph.org/. Our integrated brain data contains 1015 nodes and

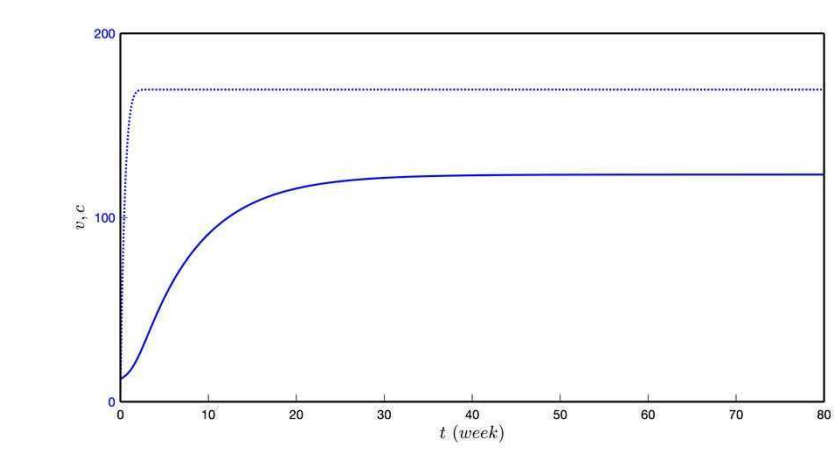

Fig. 3: (Color online) The solutions for phosphorylated tau (solid) and cognitive declines (dotted) for AD group in the presence of drug-control with $\gamma = 5.5 \times 10^{-3}, t_m = 15$ (days) and $T_p = 4p$ (weeks). The simulation uses the mean parameter values from Table 1.

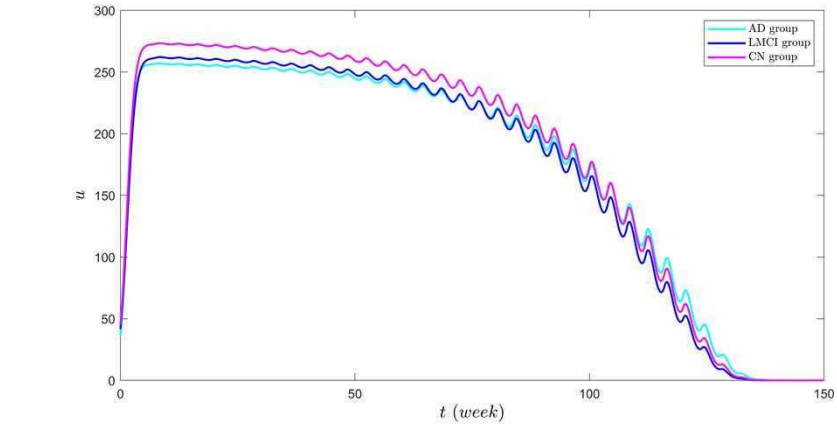

Fig. 4: (Color online) The accumulations of amyloid-beta for each group in the presence of drug-control with $\gamma = 5.5 \times 10^{-3}, t_m = 15$ (days) and $T_p = 4p$ (weeks). For each group, the simulation uses the mean parameter values from Table 1.

16,280 edges. In this brain graph data, each node corresponds to a small area (1–1.5cm^2) of the gray matter, called the region of interest (ROI). An edge may be connected with two nodes if a diffusion-MRI-based workflow finds fibers of axons running between those two nodes in the white matter of the brain [20, 21].

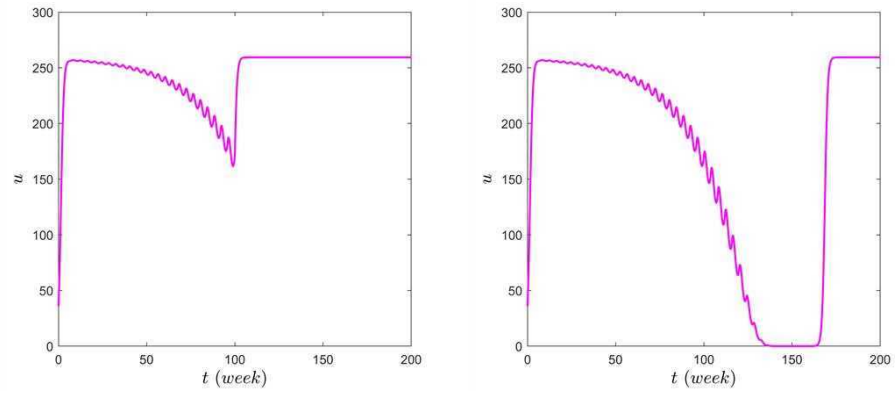

Fig. 5: (Color online) The accumulations of amyloid-beta for the AD group by applying the drug-control for a short-term (right-figure). The simulation uses the mean parameter values from Table 1 with $\gamma = 5.5 \times 10^{-3}, t_m = 15$ (days) and $T_p = 4p$ (weeks).

We have calculated the graph Laplacian based on the brain connectome data and used it in the numerical simulation of the network model. We have considered both diffusion coefficients as unity ($\rho_u = \rho_v = 1$).

At the initial stage of AD, the amyloid-beta plaque accumulates in the temporobasal and frontomedial regions in the brain connectome. On the other hand, the phosphorylated tau accumulated in the locus coeruleus and transentorhinal associated regions [see Fig. 6]. We have considered the non-zero initial values mentioned in Table 1 for amyloid-beta plaques and phosphorylated tau in these seeding sites. Furthermore, we have considered the parameter values corresponding to the AD group. Our analysis leads to the conclusion that the solution for the other groups (LMCI and CN) follows the same type of behaviours in the long term.

The developed model can potentially assist in experimental setups for Alzheimer's disease treatments. In such cases, experiments and modelling approaches enrich each other, allowing model validation strategies to be tested. Before applying the anti-amyloid beta therapy to a patient, we need to know the total number of hours/days of the drug's effectiveness. Concurrently, the time when the drug does the maximum effect on a body (e.g., t_m) is also needed. The total incubation period of a drug varies for different patients, and we find their mean (simultaneously with the standard deviation) based on the patient's age or age group. We use this mean value as the hours/days between two dosages for the patient group, i.e., the time between T_p and T_{p+1}. Recall that the mean values for the other parameter values used in our model are given in Table 1. They were initially calculated by Hao et al. [2] using empirical data from the Alzheimer's Disease Neuroimaging Initiative (ADNI) site. Integrating all this information

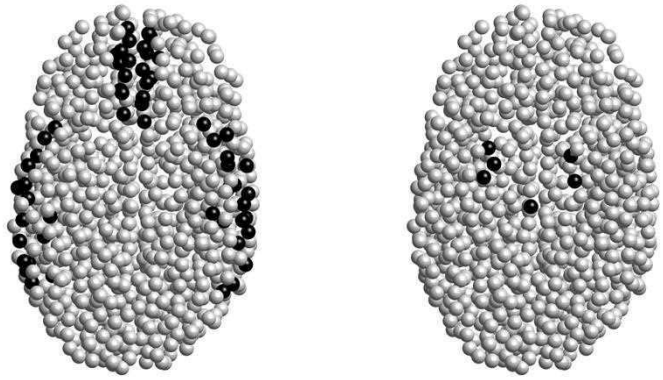

Fig. 6: (Color online) Initial seeding sites for the amyloid-beta plaques (left) and phosphorylated tau (right) in the brain connectome. Black colors represent the non-zero concentration, and gray colors represent the zero concentration.

into our mathematical model provides us with the estimate of dosages required to cure the disease and allows evaluation of each dosage's progression.

Finally, we plot the solutions for the network model corresponding to the amyloid-beta plaques and phosphorylated tau for each node presented in Fig. 7. The amyloid-beta plaque accumulation behaviours differ for different nodes at the initial stage. The accumulation grows exponentially from the starting point at some of the nodes; however, at the other nodes, it initially decreases and then increases exponentially. These behaviours depend on the degree of the nodes; a node with a higher degree distributes the plaques to all its connected nodes through diffusion, and then all of them grow exponentially. On the other hand, a node with a degree zero keeps away from others and remains unaffected all the time. The anti-amyloid-beta therapy helps to decrease the amyloid-beta plaques from all the nodes in the brain connectome.

4 Conclusions

In this paper, starting with a coupled system of reaction-diffusion equations, we have developed a model incorporating the logistic growth in the accumulation of amyloid-beta plaques and phosphorylated tau proteins. In addition, we have introduced an anti-amyloid-beta therapy in the accumulation of amyloid-beta plaques. A network mathematical model has also been considered to study the accumulations of the ingredients in the brain connectome.

We have observed that the drug function is crucial in the resulting solutions and, therefore, in developing new therapies for AD treatments. Further, a small clearance of plaques in each dosage goes towards the disease-free state

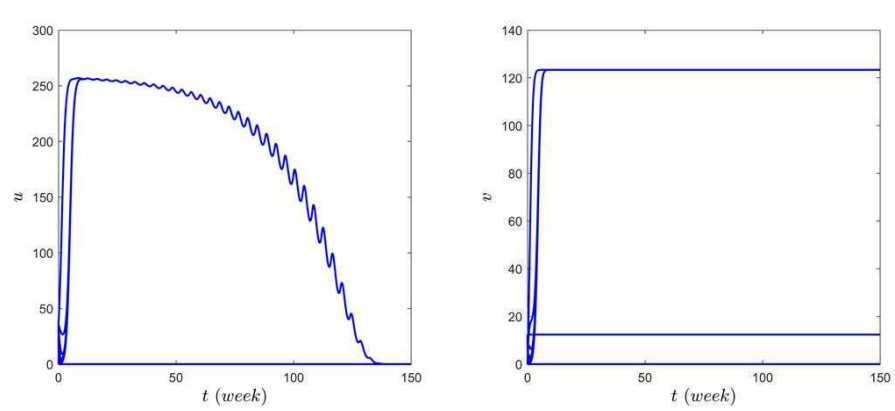

Fig. 7: (Color online) Node-wise accumulations of amyloid-beta plaques (left) and phosphorylated tau (right) for the AD group with respect to time. The simulation uses the mean parameter values from Table 1 with $\gamma = 5.5\times10^{-3}, t_m = 15$ (days) and $T_p = 4p$ (weeks).

for the long term. Our model also shows that the disease could return if we stop the medication after a particular time. Altogether, the developed modelling approach has allowed us to understand better the dynamics of drugs' clearance of the plaques that may drastically affect AD progression. Moreover, the proposed methodology can also be modified to analyze other drug-based therapies for neurodegenerative diseases.

Acknowledgements

The authors thank the NSERC and the CRC Program for their support. RM also acknowledges the support of the BERC 2022-2025 program and the Spanish Ministry of Science, Innovation and Universities through the Agencia Estatal de Investigacion (AEI) BCAM Severo Ochoa excellence accreditation SEV-2017-0718. This research was partly enabled by support provided by SHARCNET (www.sharcnet.ca) and Digital Research Alliance of Canada (www.alliancecan.ca).

References

1. Alzheimer's Association: 2020 Alzheimer's disease facts and figures. Alzheimer's Dementia, 391–460 (2020).
2. Hao, W., Lenhart, S., Petrella, J.R.: Optimal anti-amyloid-beta therapy for Alzheimer's disease via a personalized mathematical model, PLoS Comput Biol 18(9), e1010481 (2022).
3. Vaz, M., Silvestre, S.: Alzheimer's disease: recent treatment strategies, European Journal of Pharmacology 887, 173554 (2020).

4. Hardy, JA., Higgins, GA.: Alzheimer's disease: the amyloid cascade hypothesis, Science 256, 184–186 (1992)
5. Verkhratsky, A. et al.: Astrocytes in Alzheimer's disease, Neurotherapeutics: the journal of the American Society for Experimental NeuroTherapeutics 7, 399–412 (2010).
6. Panatier, A. et al.: Glia-derived D-serine controls NMDA receptor activity and synaptic memory, Cell 125, 775–784 (2006).
7. Ding, S. et al.: Enhanced astrocytic Ca2+ signals contribute to neuronal excitotoxicity after status epilepticusm, J. Neurosci. 27, 10674–10684 (2007).
8. González-Reyes, R.E. et al.: Involvement of astrocytes in Alzheimer's disease from a neuroinflammatory and oxidative stress perspective. Front. Mol. Neurosci. 10, 427 (2017).
9. Trujillo-Estrada, L. et al.: Astrocytes: from the physiology to the disease, Current Alzheimer research 16, 675–698 (2019).
10. Ackleh, A.S. et al.: A continuous-time mathematical model and discrete approximations for the aggregation of β-amyloid, Journal of Biological Dynamics 15, 109–136 (2021).
11. Bertsch, M. et al.: The amyloid cascade hypothesis and Alzheimer's disease: A mathematical model, European Journal of Applied Mathematics 32(5), 749–768 (2021).
12. Bucci, M., Chiotis, K., Nordberg, A.: Alzheimer's disease profiled by fluid and imaging markers: tau PET best predicts cognitive decline, Molecular Psychiatry 26, 5888–5898 (2021).
13. Connor, J.P., Quinn, S.D., Schaefer, C.: Sticker-and-spacer model for amyloid beta condensation and fibrillation, Frontiers in Molecular Neuroscience 15, 962526 (2022).
14. Waters, J.: The concentration of soluble extracellular amyloid-β protein in acute brain slices from CRND8 mice, PLoS ONE, 5(12), e15709 (2010).
15. Sperling. R.A.: Toward defining the preclinical stages of Alzheimer's disease: recommendations from the National Institute on Aging-Alzheimer's Association workgroups on diagnostic guidelines for Alzheimer's disease, Alzheimers Dement. 7, 280–292 (2011).
16. Haeberlein, S. et al.: Clinical development of aducanumab, an anti-abeta human monoclonal antibody being investigated for the treatment of early Alzheimer's disease, J Prev Alzheimers Dis. 4, 255–263 (2017).
17. Thompson, T.B., Chaggar, P., Kuhl, E., Goriely, A.: Protein-protein interactions in neurodegenerative diseases: A conspiracy theory, PLoS Comput. Biol. 16, e1008267 (2020).
18. Pal, S., Melnik, R.: Pathology dynamics in healthy-toxic protein interaction and the multiscale analysis of neurodegenerative diseases, In: Paszynski, M., Kranzlmüller, D., Krzhizhanovskaya, VV., Dongarra, JJ., Sloot, PM. (eds) Computational Science-ICCS 2021. Lect. Notes Comput. Sci. Springer, Cham 12746, 528–540 (2021).
19. Pal, S., Melnik, R.: Nonlocal models in the analysis of brain neurodegenerative protein dynamics with application to Alzheimer's disease, Scientific Reports 12, 7328 (2021).
20. Kerepesi, C., Szalkai, B., Varga, B., Grolmusz, V.: How to direct the edges of the connectomes: dynamics of the consensus connectomes and the development of the connections in the human brain, PLoS One 11, e0158680 (2016).
21. Szalkai, B., Kerepesi, C., Varga, B., Grolmusz, V.: High-resolution directed human connectomes and the consensus connectome dynamics, PLoS One 14, e0215473 (2019).